

# GREENHOUSE NATURAL VENTILATION BY BUOYANCY FORCES

R.Haxaire<sup>1</sup>, J.C.Roy<sup>2</sup>, T.Boulard<sup>1</sup>, M.A.Lamrani<sup>3</sup>, A.Jaffrin<sup>4</sup>

1: I.N.R.A. - Bioclimatologie, Domaine Saint Paul, 84914 Avignon Cedex 9, France

2: I.G.E. - Parc Technologique, 2, av. J.Moulin, 90000 Belfort, France

3: Laboratoire de Thermodynamique - Université Ibnou Zohr, BP 28/S Agadir, Maroc

4: UR1H-SRIV, I.N.R.A. - Centre d'Antibes, Sophia Antipolis, 06410 Biot, France

## Abstract

Convective transfers mainly determine the energy and mass balances which regulate the micro-climate inside a greenhouse. Air flow and temperature patterns induced by natural ventilation through greenhouse roof openings are only considered here. Flow visualizations were performed on a half scale test cell simulating the absorption of solar radiation at the floor surface of a single-span greenhouse. Temperature and air flow patterns were observed in a steady regime i) with a single sided roof vent and ii) with two symmetrical one. An air inflow always take place at the lower part of the openings and feed a single convective loop which follows the walls of the greenhouse before escaping through the upper part of the vents. These natural convective patterns were numerically simulated by means of a Computational Fluid Dynamic code (CFD 2000<sup>TM</sup>). It was found that the convective cell, velocity values and the temperature profiles were generally in good agreement with the experimental results.

**Keywords:** Greenhouse, natural convection, ventilation

## 1 Introduction

Natural convection in greenhouses determines the inside aerodynamic and thermal patterns and the transpiration and photosynthesis rates of the canopy. Natural ventilation combines buoyancy and wind effects as driving forces. When the wind is low, the buoyancy forces are important. It is the case during day time, when they are crucial for greenhouse cooling. Up to now, most studies on natural ventilation were based on global air exchange rates deduced from tracer gas measurements which offer no details on internal flow patterns and temperature profiles (Fernández and Bailey, 1992; Boulard and Draoui, 1995; Kittas et al., 1995). More generally, detailed air motions driven by wind or buoyancy effects inside greenhouses remain poorly known. Consequently, most authors assume homogeneity for the air (Kindelan, 1980; Kimball, 1986; de Halleux et al., 1991) and a unique air temperature and velocity are considered in the whole greenhouse volume. Recent progress in flow modeling by means of computational fluid dynamics programs (CFD) allows an easier access to vectors and scalars by solving transport equations in closed (Boulard et al., 1997; Lamrani, 1997) and ventilated (Mistriotis et al., 1997) greenhouses. The accurate experimental investigation of buoyancy effects in a full scale greenhouse is a more complicated task because air flows are turbulent even at low velocities. This is why few studies were devoted in the past years to internal convective loops. Authors mainly consider natural convection generated by local heat sources in a closed mono-span greenhouse (Carpenter and Bark, 1967) or natural ventilation by buoyancy forces due to a slightly open overhead vent (Gray, 1954). However, these results are merely qualitative and do not allow any comparison between experimental data and simulated results. Steady state conditions with well defined boundary conditions offer such an opportunity, as shown by laboratory experiments performed on scale structures by Nara (1979) and Lamrani (1997). In these conditions, even simple measurements can provide useful hints on flow patterns and temperature profiles. The purpose of this paper is to provide detailed information about natural ventilation induced by thermal effects in a greenhouse equipped with roof vents. It will combine an experimental study in a

half-size model scale greenhouse and a simulation study by means of a Computational Fluid Dynamic software.

## 2 Material and Methods

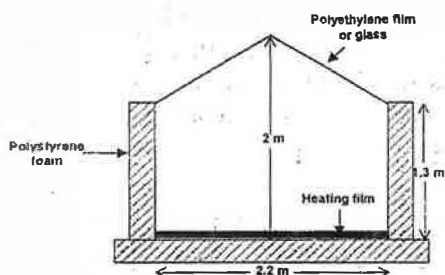


Figure 1: The half scale greenhouse model

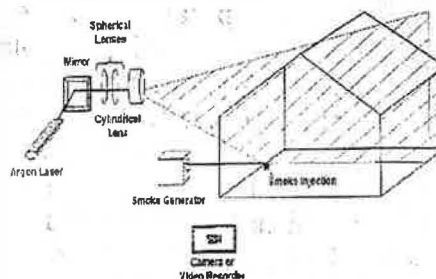


Figure 2: The laser tomography system

### 2.1 Experimental set-up

To generate a steady-state regime, experiments were performed in well controlled artificial conditions. We focused on a situation characterized by absorption of the largest part of the incident solar radiation at soil level. In these conditions, widely observed in greenhouses, the soil surface is warmer than the roof and the walls. These steady-state boundary conditions were created inside a reduced scale greenhouse by electrically heating its floor at a constant flux and by cooling its roof and walls at constant temperature in an air-conditioned obscure hall with large thermal inertia. The greenhouse was equipped with vents on both roof slopes (figure 1).

#### Similitude conditions

The similitude condition for natural convection between the reduced scale (rs) and a full scale (fs) greenhouse is the conservation of the Rayleigh number. The definition of the Rayleigh number,  $Ra$ , relative to a heated enclosure of dimension  $l$  and temperature gap  $\Delta T$  between the warm and cold surfaces or media is:

$$Ra_{rs} = Ra_{fs} = \frac{g \cdot \beta \cdot \Delta T \cdot l^3}{\nu \cdot a} \quad (1)$$

Where  $g$  is the gravity constant,  $\beta$  the thermal expansion coefficient,  $\nu$  the cinematic viscosity, and  $a$  the thermal diffusivity of air.

Considering air as the fluid medium will then give the relation between geometric and thermal characteristics of the reduced and full-scale greenhouses:

$$\frac{l_{fs}}{l_{rs}} = \left( \frac{\Delta T_{rs}}{\Delta T_{fs}} \right)^{\frac{1}{3}} \quad (2)$$

As a two degrees air temperature difference between the inside and the outside of a greenhouse can be typically observed during summer time, a difference of sixteen degrees would then be required in the reduced greenhouse, following equation 2, to reproduce the real convection pattern without distortion in a half-size model scale greenhouse ( $\frac{l_{fs}}{l_{rs}} = 2$ ).

#### The reduced scale greenhouse

The reduced scale mono-span greenhouse was 2.2 m wide, 2 m high and 1.5 m long (figure 1). An heating film covered the floor and provided, at full power ( $300 \text{ W} \cdot \text{m}^{-2}$ ), thermal conditions consistent with a scale factor of 0.57. The roof slopes were covered with a polyethylene film to minimize the absorption of the radiative heating from the floor. To imitate physical conditions occurring in a long greenhouse and to prevent three dimensional flow patterns, the side walls and gables were thermally insulated by means

of 6 mm double wall polycarbonate sheet covered by 5 cm closed cell polystyrene foam. Two continuous vents (1.5 m length x 0.65 m width) could tilt the lower half of the roof slopes from the level of the gutter on both sides (figure 1), up to the horizontal position (H, the opening height = 0.38 m).

### Temperature measurements

Air and surfaces temperatures in the model greenhouse were measured by means of very thin thermocouples ( $\phi = 0.2$  mm) placed along a grid with a 20 cm x 25 cm mesh. The density was increased near the vent openings, the walls, the floor and the roof. All together, 44 probes were used for air temperatures, and 6 probes for surface temperatures. In addition, we designed two special combs featuring five thin ( $\phi = 0.2$  mm) thermocouples with a 2 cm spacing, to investigate air temperature patterns in the vicinity of the wall surfaces and in the vent opening. All the data were sampled at a frequency of 1 Hz, then averaged and recorded in two data loggers before being processed.

### Air flow characterization

Direct visualization techniques by laser tomography, which are non intrusive methods, have been used to map out flow fields. The experimental set-up is shown in figure 2. The Laser beam produced by an Argon Laser is enlarged in two-dimensions by means of lens in order to obtain a laser sheet. The laser light reflected by the oil-droplets produced by a smoke generator reveals a complete picture of the flow. Though quantitative data can be extracted from these pictures using image processing, most of our observations were purely qualitative. The quantitative flow measurements in the central vertical plane of the greenhouse were determined using an other method: a unidirectional hot wire anemometer (Dantec Flow-master). The velocity sensor was mounted on a long (2.5 m) and thin metallic rod ( $\phi = 0.8$  cm), allowing XY-displacements for the investigation of the entire vertical central plane of the greenhouse without disturbing of the flow. For each position along the grid, the average vertical and horizontal velocity components were successively measured during periods of two minutes and recorded by a specific software.

## 2.2 Simulations

### Numerical computation

The Bernoulli's relation, widely used to evaluate the overall ventilation rate of greenhouses, don't allow for the determination of the climate spatial heterogeneity.

A numerical resolution of the conservative equations of mass, momentum and energy is necessary to have access to the distributed climate. A commercial Computational Fluid Dynamic software was used: CFD2000<sup>TM</sup>. It uses a finite volumes code, the PISO numerical method (Issa, 1985) to solve the set of transport equations.

As in a 3 m high greenhouse the flow is turbulent when the temperature difference between the soil and the roof is greater than 0.1 °C, a standard two equations  $k - \epsilon$  model assuming isotropic turbulence was chosen to describe the turbulent transports. This modeling of turbulence was preferentially selected for this application as it is a compromise between level of sophistication and computational efficiency (Jones and Whittle, 1992).

### Mesh and boundary conditions

To limit our control volume around the model-scale greenhouse, we have chosen pressure-type boundary conditions around the greenhouse. These boundary conditions prescribed fixed pressure and temperature conditions at the limits of the computational domain and the inlet and outlet speeds are automatically computed to satisfy the continuity. Imposed temperature conditions (equivalent to the measured values) are applied at floor and roof levels and adiabatic conditions are selected for the walls in order to simulate their insulation by polystyrene foam. Body fitted irregular Cartesian meshes was used to conform the grid exactly to the contours of the boundary conditions. The driving forces of natural convection are buoyancy forces arising from small temperature differences within the flow according to the Boussinesq hypothesis.

## 3 Results

### 3.1 Speed and temperature fields measurement

#### Single sided roof opening

The pattern of mean air flows, as measured by hot wire anemometry, is shown in figure 3. The air flow is characterized by a strong recirculation rate with a rotating air loop showing the highest speed values at the opening ( $0.4 \text{ ms}^{-1}$ ) and along the walls ( $0.3 \text{ ms}^{-1}$ ). Still air conditions prevail in the center of the greenhouse. The corresponding air temperature pattern is shown in figure 5. From the floor surface up, the temperature decreases by about 20 degrees in the first 5 cm, and then remains almost unchanged over the whole height of the inner volume, before decreasing slightly again in the last 25 cm below the roof surface. The main temperature gradients are localized along the walls and gusts of cold air from the outside flow around the lower edge of the roof opening and trickle down the side wall, before being warmed up at the floor level. On the opposite side, gusts of warm air coming from the floor rise along the adiabatic left wall and sweep the roof where they cool down, before escaping from the greenhouse through the upper part of the vent.

#### Two sided ventilation

The pattern of average air flows for a similar Raleigh number is shown in figure 7. Despite the symmetrical position of the two vents, the air motion was characterized by a single rotating air loop which breaks this symmetry. Air from the outside enters through the lower part of the right opening and, for a weaker part, through the lower part of the left opening. The inner air loop separates into two parts, one part leaving the greenhouse through the upper part of the left opening, while the major part keeps rotating before escaping in part through the upper part of the right side opening. As previously, the highest air speed are observed in the vent opening (up to  $0.27 \text{ ms}^{-1}$  in the right side vent) and along the walls, with stagnant conditions in the core of the greenhouse. The corresponding air temperature pattern is shown in figure 9. Air temperature decreases by about 19 degrees (on the left side) in the first 5 cm above the heating floor, and then remains almost unchanged over the whole height of the volume. Gusts of cold air flowing in the greenhouse through the lower part of the right side opening are then warmed up at the floor level. Contrary to the case of a single opening, there is clearly an inflow of cold air coming from the outside through the left vent which cools down the flow.

### 3.2 Numerical results

#### Single sided roof opening

Calculation with the CFD software were performed using a  $62 \times 56$  grid with a refinement of the mesh along the walls. The thermal boundary conditions were imposed surface temperature corresponding to the values which were measured in the experiments. Figures 4 and 6 show calculated air flows and isotherms. As in the experiment velocity vectors show that an essentially single circulation pattern prevails with the highest speeds along the walls and the lowest in the core of the cavity and in the corners between the floor or the roof and the walls. The order of magnitude of the air speed vectors is also similar to the observed values (21.8 against  $19 \text{ cm/s}$  from 20 cm of the floor). Temperatures contours (figure 6) display also absolute values and a distribution which is very similar to the measured field.

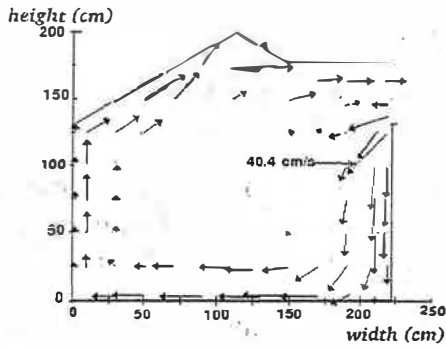


Figure 3: Measured velocities with a single sided vent opening:  $Ra = 6.6 \cdot 10^6$

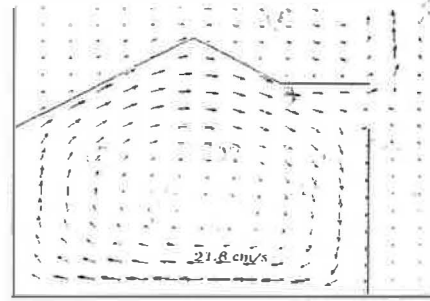


Figure 4: Computed velocities with a single sided vent opening:  $Ra = 6.6 \cdot 10^6$

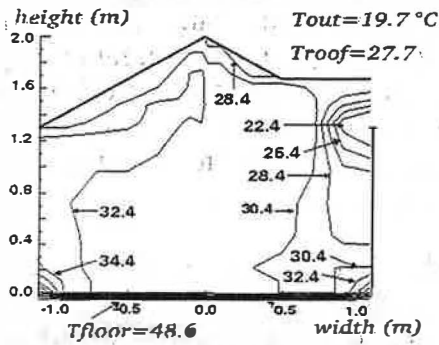


Figure 5: Measured temperature pattern with a single roof-vent:  $Ra = 6.6 \cdot 10^6$

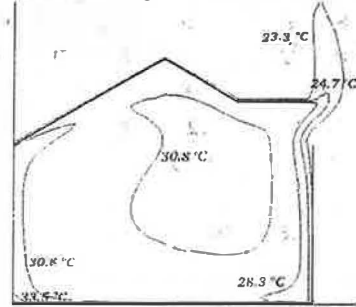


Figure 6: Computed temperature pattern with a single roof-vent:  $Ra = 6.6 \cdot 10^6$

### Two sided ventilation

A  $78 \times 52$  grid with a refinement of the mesh along the walls was chosen for the case with two openings. The thermal boundary conditions were also chosen to be similar to the experimental ones. Calculated air flow and temperature patterns are shown in figures 8 and 10. As in the experiment and despite the symmetrical position of the two vents, the air motion is characterized by a single rotating air loop. More generally, we can observe that both the temperature contours and the flow patterns display a distribution which is similar to the measured fields.

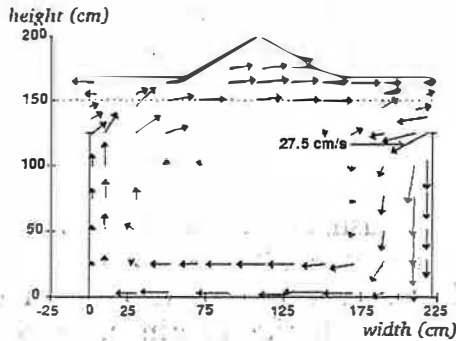


Figure 7: Measured velocities with a two sided vents opening:  $Ra = 6.6 \cdot 10^6$

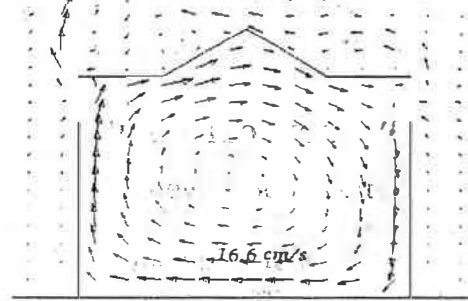


Figure 8: Computed velocities with a two sided vents opening:  $Ra = 6.6 \cdot 10^6$

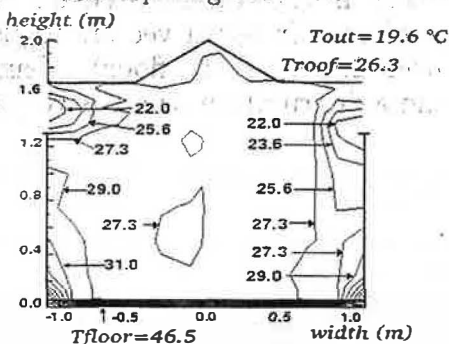


Figure 9: Measured temperature pattern with a two sided roof-vents:  $Ra = 6.6 \cdot 10^6$

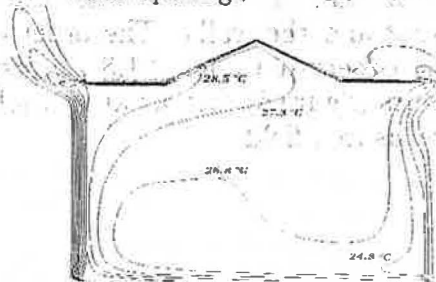


Figure 10: Computed temperature pattern with a two sided roof-vents:  $Ra = 6.6 \cdot 10^6$

## 4 Conclusion

The air flow and temperature patterns generated by ventilation by buoyancy forces were experimentally studied in a half scale mono span greenhouse with a moderate temperature differences between a heating floor, simulating the absorption of solar radiation, and outside air. The air flow and temperature fields were studied by means of techniques combining temperature measurements, using thermocouples, and flow visualization by laser tomography and measurements by hot wire anemometer. A commercial CFD software with finite elements schemes and standard  $k - \epsilon$  turbulent model; CFD2000<sup>TM</sup> was also used to simulate the air flow and temperature patterns generated by buoyancy forces with exactly the same boundary conditions than in the experimental ones.

For a single-sided roof opening, the air motion is characterized by a single air loop with high air speed along the floor, walls an roof and still conditions in the core of the greenhouse. The air flows in the lower part of the vent opening and flows out through the upper part of the same vent opening. For a two-sided ventilation, the flow pattern always exhibited a single loop and outside air came in through the lower part of the two vents and flows out through their upper part. In both cases, the thermal boundary layer only extend over a small distance (5 to 6 cm) whereas velocity gradient extended much farther, 50 cm away from the walls.

When compared to the classical approaches of ventilation phenomena based on the hypothesis of homogeneity of the inside air, these new experimental and simulation approaches allow to determine the spatial heterogeneity of both vector and scalar fields. It is a first step toward the determination of the climate distribution at the plant level and it is planned, in a near future, to study the influence of plants on the flow field and to simulate it by means of the porous medium approach.

## References

- Boulard, T. and Draoui, B. (1995). Natural ventilation of a greenhouse with continous root vents: measurement and data analysis. *Journal of Agricultural Engineering Research*, 61:27–36.
- Boulard, T., Roy, J., Lamrani, M., and Haxaire, R. (1997). Characterising and modelling the air flow and temperature profiles in a closed greenhouse in diurnal conditions. In IFAC, editor, *Mathematical and Control Applications in Agriculture and Horticulture, Hannover, Germany*.
- Carpenter, W. and Bark, L. (1967). Temperature patterns in greenhouse heating. *Florists' Rev.*, 139:17–19.
- de Halleux, D., Nijskens, J., and Deltour, J. (1991). Adjustment and validation of a greenhouse climate dynamic model. *Bull. rech. Agrono. Gembloux*, 26(4):429–453.
- Fernández, J. and Bailey, B. (1992). Measurement and prediction of greenhouse ventilation rates. *Agricultural and Forest Meteorology*, 58:229–245.
- Gray, H. (1954). Greenhouse heating. *Cornell Agric. Exp. Sta. Bul.*, 906.
- Issa, R. (1985). Solution of the implicitly discretized fluid flow equations by operator-splitting. *Journal of Computational physics*, 62:40–65.
- Jones, P. and Whittle, G. (1992). Computational fluids dynamics for building air flow prediction - current capabilities. *Building and Environment*, 27(3):321–338.
- Kimball, B. (1986). A modular energy balance program including subroutines for greenhouses and the other latent devices. *Agricultural Research Service*.
- Kindelan, A. (1980). Dynamic modelling of greenhouse environnement. *Transaction of the ASAE*, 5:1232–1239.
- Kittas, C., Draoui, B., and Boulard, T. (1995). Quantification of the ventilation of a greenhouse with a roof opening. *Agricultural and Forest Meteorology*, 77:95–111.
- Lamrani, M. A. (1997). *Characterisation and modelling of the natural laminar and turbulent convection and ventilation in a greenhouse*. PhD thesis, University of Agadir.
- Mistriotis, A., Bot, G., and Scarascia-Mungnozza, G. (1997). Analysis of the efficiency of greenhouse ventilation using computational fluid dynamics. *Agricultural and Forest Meteorology*, 85:217–228.
- Nara, M. (1979). Studies of air distribution in farm buildings. *The Journal of the Society of Agricultural Structures*, 9(2):17–26.